AFRL-SR-BL-TR-99-

0203

REPORT DOCUMENTATION PAGE

1. AGENCY USE ONLY (Leave Blank)	2. REPORT DATE 25 May 99	3. REPORT TYPE AND DATES COVERED Final From 09/01/98 to 02/28/99

4. TITLE AND SUBTITLE
Flexible Polymer Modulators for Large Conformal Antenna Arrays

5. FUNDING NUMBERS
F49620-98-C-0059

6. AUTHORS
B. Tsap,
L.R. Dalton, W.H. Steier
H.R. Fetterman

7. PERFORMING ORGANIZATION NAME(S) AND ADDRESS(ES)

Pacific Wave Industries, Inc.
10911 Weyburn Ave., Suite 222
Los Angeles, CA 90024

University of Southern California
University Park
Los Angeles, CA 90089

8. PERFORMING ORGANIZATION REPORT NUMBER
1

9. SPONSORING / MONITORING AGENCY NAME(S) AND ADDRESS(ES)
Dr. Charles Lee,
AFOS/PKA
801 N. Randolph St., Room 732
Arlington, VA 22203-1977

10. SPONSORING / MONITORING AGENCY REPORT NUMBER

19990903 116

11. SUPPLEMENTARY NOTES

DE

12a. DISTRIBUTION / AV.

13. ABSTRACT (Maximum 200 words)

Report developed under STTR contract. Polymer electro-optic modulators were fabricated on flexible Mylar substrates, which will serve as one of the main building blocks for the future optically-controlled antenna arrays. The fully operational devices exhibited modulation properties at W-band similar to the devices on rigid substrates and are expected to demonstrate comparable performance at other frequencies of interest. Use of Mylar substrates will allow us to commercialize modulators with integrated finline-rectangular waveguide transitions working up to 100 GHz. Other major advances have been achieved by successfully designing, fabricating, and testing photonic RF phase shifters. They consisted of two nested Mach-Zehnder modulators and exhibited an RF phase shift of over 100 degrees at 16 GHz with a DC-control voltage change of 7.8 V. This project has not not only demonstrated the ability of our exicting technology to fabricate complex closely placed electro-optic polymer components on flexible substrates, but also opened the entirely new way of implementing photonically-controlled phased arrays.

14. SUBJECT TERMS

STTR Report	Flexible Mylar Substrate	Photonic RF Phase Shifter
Optical Modulator	Nested Mach-Zehnder Configuration	Riged Optical Waveguide
High Frequency Response	Finline Transition	

15. NUMBER OF PAGES
21

16. PRICE CODE

17. SECURITY CLASSIFICATION OF REPORT Unclassified	18. SECURITY CLASSIFICATION OF THIS PAGE Unclassified	19. SECURITY CLASSIFICATION OF ABSTRACT Unclassified	20. LIMITATION OF ABSTRACT UL

DTIC QUALITY INSPECTED 4

DISTRIBUTION STATEMENT AUTHORIZATION RECORD

Title: *Flexible Polymer Modulators for Large Conformal Antenna Arrays*

Authorizing Official: *DR. Charles Lee*

Agency: *AFOSR* Ph. No. *(703) 696-7779*

☐ Internet Document: URL: _____
(DTIC-OCA Use Only)

Distribution Statement: (Authorized by the source above.)

☒ **A:** Approved for public release, distribution unlimited.

☐ **B:** U. S. Government agencies only. (Fill in reason and date applied). Other requests shall be referred to (Insert controlling office).

☐ **C:** U. S. Government agencies and their contractors. (Fill in reason and date applied). Other requests shall be referred to (Insert controlling office).

☐ **D:** DoD and DoD contractors only. (Fill in reason and date applied). Other requests shall be referred to (Insert controlling office).

☐ **E:** DoD components only. (Fill in reason and date applied). Other requests shall be referred to (Insert controlling office).

☐ **F:** Further dissemination only as directed by (Insert controlling DoD office and date), or higher authority.

☐ **X:** U. S. Government agencies and private individuals or enterprises eligible to obtain export-controlled technical data in accordance with DoD Directive 5230.25.

NOTES: _____

_____

_____

_____

J. Keith _____ *1 Oct 99*
DTIC Point of Contact   Date

Table of Contents

i. Introduction

Recently there has been considerable interest in designing and developing large antenna arrays for aircraft. The arrays are formed from composite layers which may contain conformal radar, conformal microstrip or spiral antennas for electromagnetic applications. The use of fiber-optic control of phased array antennas has been proven to dramatically reduce size and weight of these antenna systems. Integration of different optical component, such as lasers, photodiodes, modulators, optical waveguides and interconnects on flexible substrates will give a boost to the development of optically controlled large conformal antennas.

Several key components, which may be used for optical control and steering of conformal antenna arrays, have been demonstrated in the past decade. They include, but are not limited, to polymeric light emitters and detectors, modulators, and electronic and photonic interconnects.

The current advances of USC and PWI researchers in the development of stable materials containing acentrically ordered organic chromophores and high frequency nonlinear polymer modulators open real possibilities for the development of viable prototypes for optically interconnected conformal phased array systems. Integration of these components on flexible substrates is vital to implementing optically controlled electronics for large area antennas.

In this Phase I, we fabricated and tested polymer electro-optic modulators on flexible mylar substrates, which will serve as one of the main building blocks for the future conformal antenna arrays. Mylar, the material of choice was utilized because of its microwave properties, chemical stability, and full compatibility with our existing polymer processing and photolithography techniques. The fully operational devices exhibited modulation properties at W-band similar to the devices on rigid substrates and are expected to demonstrate comparable performance at the other frequencies of interest.

Another major advance in the development of polymer photonic components has been achieved during this Phase I STTR project. We successfully designed, fabricated, and tested a photonic RF phase shifter. It consisted of two nested Mach-Zehnder modulators, and exhibited a RF phase shift of over 100 degrees at 16 GHz with a DC-control voltage of 7.8 V. This project has not only demonstrated the ability for our existing technology to fabricate complex closely placed electro-optic polymer components, but also opened the entirely new way of implementing photonically-controlled phased array antennas.

We also adapted the commercial High Frequency Structure Simulation program for evaluating complex three dimensional optical waveguide structures. It allowed us to perform rigorous computer simulations to evaluate performance of polymer electro-optic and passive components on flexible substrates. Results of these simulations may be used for optimization of the adapted device structures, which we expect to fabricate in the next phase.

3

1. Fabrication and Investigations of Polymer Modulators on Mylar Substrates

The development and improvement of inexpensive broad bandwidth low half-wave voltage, V_π, optical modulators is crucial to the implementation of several photonic systems. These include optical control of phased arrays, optical distribution of voice, data, and video services, and the fabrication of higher complexity photonic components from different modulator configurations. Some of these components are photonic RF phase shifters, switches, and polarization selective couplers. Over the past several years high performance rigid modulators have been demonstrated. However, the demand for conformal systems to be used in "smart skin" structures has placed pronounced emphasis on the development of flexible modulators and other photonic components.

During our phase I effort arrays of polymer traveling-wave phase modulators were fabricated on flexible Mylar substrates and their high frequency characteristics were investigated under conditions which involved no flexing. These devices were integrated with antipodal to microstrip transitions enabling the modulator to be driven by waveguide components, which effectively covered W-band (75 – 110 GHz). Furthermore, different optical coupling schemes were examined in an attempt to maximize coupling. Our future efforts in the arena of flexible photonic polymeric devices will include comprehensive investigations of flexible polymer modulators under flexed conditions and the fabrication of higher complexity photonic devices from different configurations of flexible polymer modulators. In particular, issues of optical confinement in flexed polymer optical waveguides will be studied and resolved. Furthermore, in order to capitalize on the full potential of flexible modulators, the frequency response of flexed polymer modulators will be investigated and optimized. Our plans for implementation of higher complexity photonic devices can be found on subsequent sections.

During our phase I effort several flexible substrates were examined and were required to meet certain physical, electrical, and chemical characteristics. These were thermal stability and reasonable thermal conductivity at temperatures exceeding 150 °C, sufficient mechanical support for films approximately 100 μm thick, low dielectric losses at microwave frequencies, low dielectric constant to prevent loading of the millimeter wave waveguide, and chemical compatibility with the polymer modulator fabrication process. Among the substrates studied Mylar was found to most closely match our requirements. Therefore, arrays of flexible polymer phase modulators were fabricated on 127 μm thick Mylar substrates. The Mylar film was glued onto a Silicon wafer for mechanical support during our standard fabrication procedure, Figure 1 shows a schematic of this process. Prior to device fabrication, layers of Ag and Au were deposited on the Mylar substrate to form the ground plane for the microstrip line.

The flexible polymer modulator fabrication procedure consisted of the following steps. Using standard photolithography techniques, the lower finline transition was patterned and subsequently etched in the region to be inserted in the millimeter wave waveguide.

4
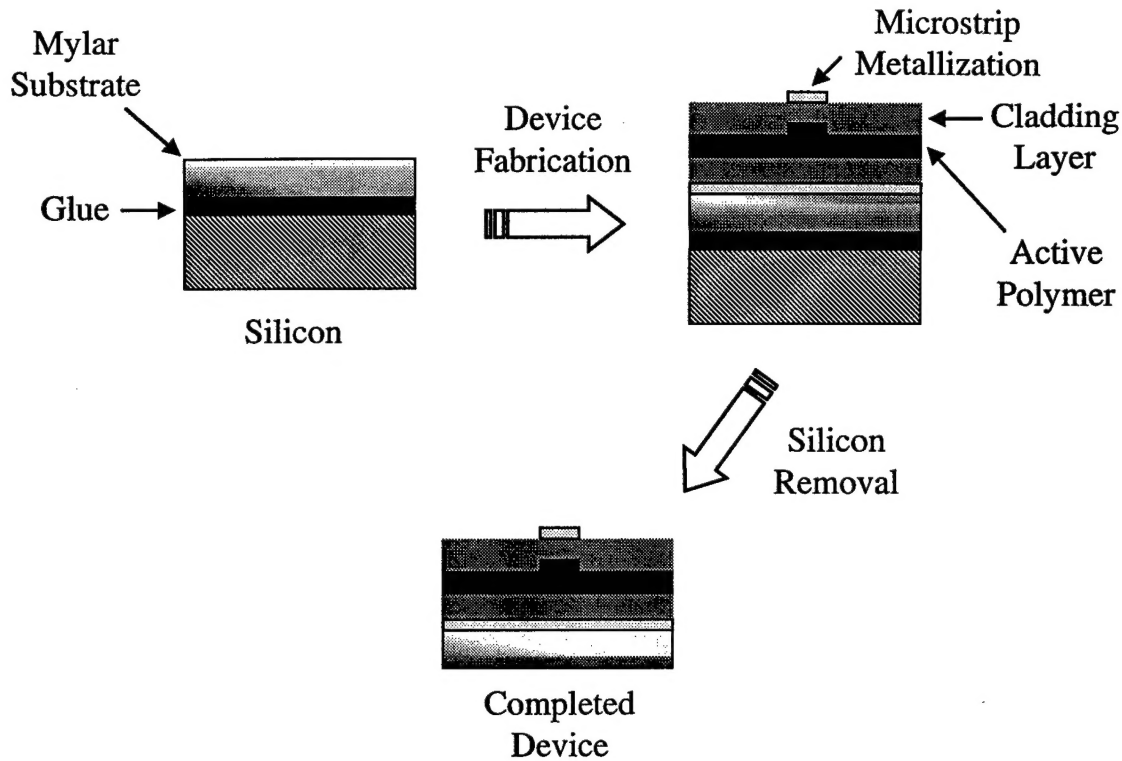
Figure 1. Schematic representation of polymer traveling-wave modulator fabrication on a Mylar substrate.

The lower cladding and active polymer, APII, layers were then spin coated on the substrate and the active polymer was corona poled. The APII active polymer has demonstrated an electro-optic coefficient of 30 pm/V. The optical waveguide ridge was then defined using reactive ion etching (RIE). The upper cladding was spun on and a thin layer of Cr and Au was deposited for the top electrode. A thick photoresist layer was then patterned to define the top electrode and the upper finline transition region. This pattern was precisely aligned to both the polymer optical waveguide and the lower finline. Electrochemical gold plating was used to increase the thickness of the top gold electrode to 7 μm. The ends of the optical waveguide were then prepared by dicing. Figure 2a shows a picture of the completed device. The particular finline transition region to be inserted into the rectangular waveguide was separated from the array and the polymer layers on the lower finline transition pattern removed using a solvent that was locally applied. The transition was then inserted into the waveguide. Figure 2b shows a picture of the packaged device.

Figure 3 shows the polymer modulator high frequency characterization setup. Although, a Mach-Zehnder modulator is shown in the canonical representation of the setup, it was capable of characterizing both phase and intensity modulators. A diode pumped Nd:YAG laser operating at 1310 nm(or equivalently at a frequency Ω_1) was butt-coupled
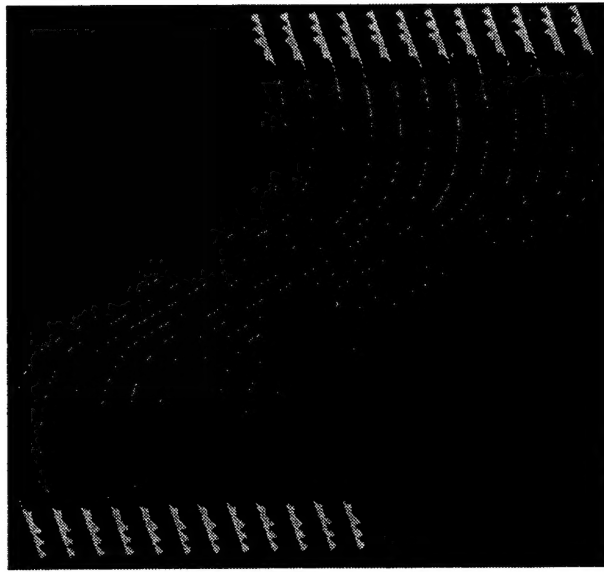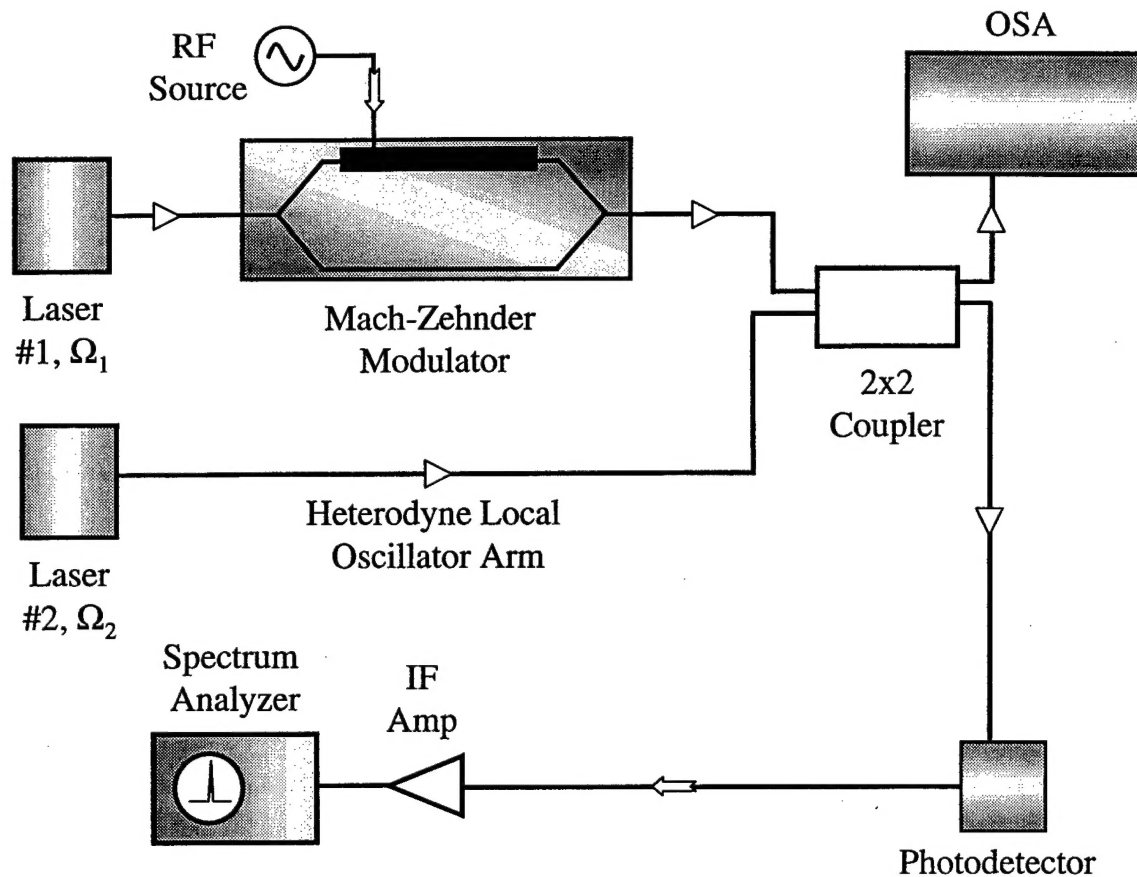
a)
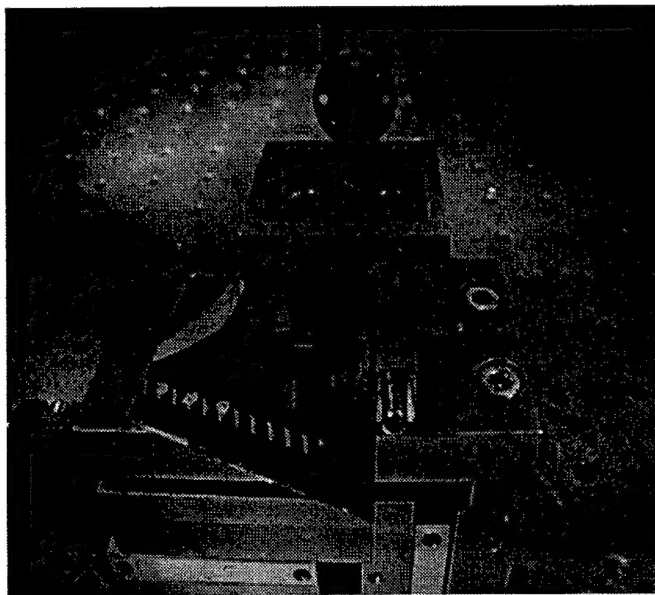
b)

Figure 2. a) Picture of completed flexible polymer traveling-wave phase modulator with finline to microstrip transitions. b) Picture of packaged flexible polymer phase modulator. A W-band waveguide acts as the driver for one of the devices.

6

Figure 3. Schematic representation of the polymer traveling-wave modulator high frequency characterization setup. In this case Ω_1 and Ω_2 represent the respective laser frequencies.

to the optical waveguide endface of the modulator using single mode PM fiber. The local oscillator optical beam was derived from an external-cavity semiconductor diode laser, which could be tuned several hundred GHz about the Nd:YAG laser frequency. Fine tuning of the difference frequency, Ω_1-Ω_2, was achieved by precisely adjusting the frequency of the Nd:YAG laser. Furthermore, the modulator drive consisted of a W-band millimeter wave source. Both beams were combined using a 2x2-fiber coupler and fed to a fast photodetector, the output of which was measured using a HP microwave spectrum analyzer. The difference frequency of the two laser beams was monitored using a HP optical spectrum analyzer.

The heterodyne technique previously described provided information of the modulator frequency response at the millimeter wave frequency at which it was driven. The signal detected by the spectrum analyzer was proportional to

$$E_m E_o \cdot \frac{\pi V_m}{V_\pi(f)} \cdot \sin\left\{2\pi \cdot \left(f - \left(\Omega_1 - \Omega_2\right)\right) \cdot t\right\} \tag{1}$$

where E_m and E_o were the optical field amplitudes from the modulator and local oscillator respectively, f was the millimeter wave frequency, V_m was the amplitude of the millimeter wave driving the modulator, and $V_\pi(f)$ was the effective half-wave voltage at the millimeter wave frequency. The amplitude of the frequency response of the modulator could be extracted from the amplitude of the signal measured by the spectrum analyzer, which in turn was inversely proportional to $V_\pi(f)$.

For the characterization of the flexible polymer traveling-wave phase modulator, a 50 mW GUNN diode operating at 95 GHz was used to drive the device and the frequencies of the lasers were separated by approximately 90 GHz. The signal measured by the spectrum analyzer under these conditions is shown in Figure 4. It exhibited a -42 dBm power level with a signal to noise ratio of 11 dB. These results were comparable to those previously reported at W-band for rigid polymer traveling-wave phase modulators. These are particularly encouraging results for a phase modulator that has a V_π of 16 V. Note that this corresponds to a half wave voltage of 10.6 V if the modulator assumes a Mach-Zehnder architecture and 5.3 V if the Mach-Zehnder is realized in a push-pull configuration. Fabrication procedures for the realization of push-pull Mach-Zehnder modulators are currently under intensive investigation.
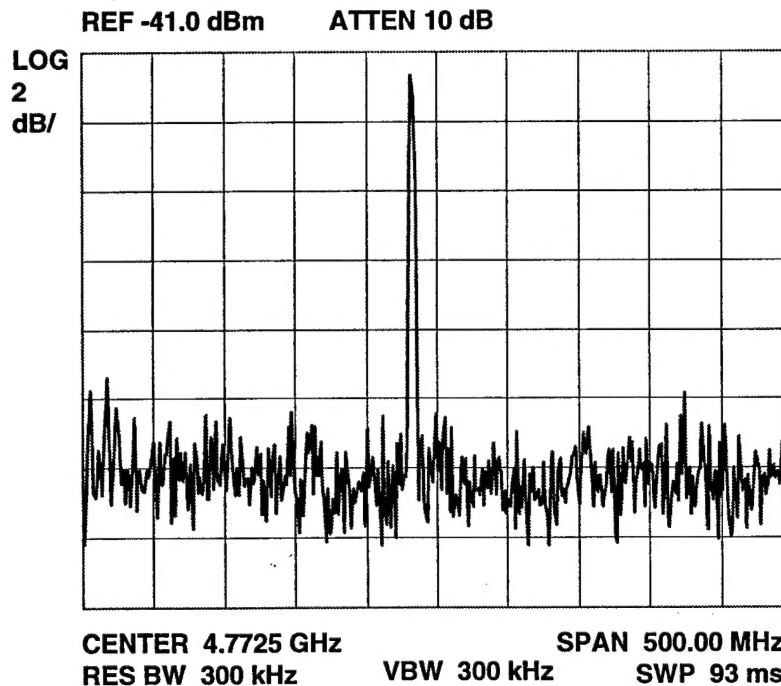
Figure 4. Flexible polymer modulator response at 95 GHz measured by the spectrum analyzer.

Lastly, during our phase I effort we initiated an examination of optical coupling optimization, which is a significant issue in the operation of waveguide modulators. Our examination consisted of a comparison of the coupling loss obtained for different optical

fiber types. Single mode fibers with 9.3 and 3.2 μm field mode diameters and single mode lensed fibers were investigated. Although, the 3.2 μm field mode diameter fiber provided some improvement in coupling loss over the 9.3 μm one, the single mode lensed fiber demonstrated the best performance. The lensed fiber showed coupling loss improvements over the other fiber types by up to 6 dB. These encouraging results have prompted the expectation of future pig-tailing of flexible polymer modulators to lensed fibers.

Using our mature polymer device fabrication technology, we have demonstrated the fabrication of polymer traveling-wave modulators on flexible substrates. These devices exhibited high performance levels in terms of frequency response as confirmed by our W-band measurements. Future investigations and optimizations of flexible polymer modulators under flexed conditions will yield the necessary knowledge to make feasible the realization of fully integrated conformal photonic systems.

2. Fabrication and Investigations of Polymeric Photonic RF Phase Shifters on Flexible Substrates

Photonic RF phase shifters (PPSs) have received and continue to receive considerable attention in the research arena, particularly in connection with phased arrays and their beam forming function. This persistent attention arises from the significant advantages offered by integrated photonics to phased array systems, which include low cost, low power consumption, and lightweight. However, most of the PPSs investigated to date have been fabricated from $LiNbO_3$ precluding the fabrication of flexible devices. In the previous section we described polymer modulators fabricated on flexible substrates with performance comparable to those fabricated on rigid ones. Therefore, based on our phase I results, fabrication of flexible PPSs seems immediately realizable.

As part of our continued effort in flexible polymeric devices, we will extend the fabrication of the RF PPS we examined in our phase I work to Mylar substrates. Thereby imparting the advantages of a flexible substrate to the photonic phase shifting function. These advantages include conformal properties, robustness, and minimal loading of the microwave waveguide at W-band. To fully utilize the conformal properties made possible by the flexible substrate and the polymeric nature of the device, experimental investigations of the RF PPS under flexed conditions are necessary. In particular, the effect of optical and microwave waveguide bending on the microwave phase shifting function will be determined. Furthermore, we have identified that the PPS configuration investigated during our phase I is addressable (may be switched between two modes, which eliminates additional RF switching components) and as such lends itself to implementation in more complex systems. Our plans and expectations for a flexible substrate RF PPS are founded on the encouraging results yielded by our phase I efforts.

During this effort, we employed our mature polymer device fabrication technology in the realization of an RF PPS, a schematic of which is shown in Figure 5a. The photonic phase shifter was configured from two nested Mach-Zehnder modulators, which demonstrated our ability to integrate basic photonic devices to form higher complexity
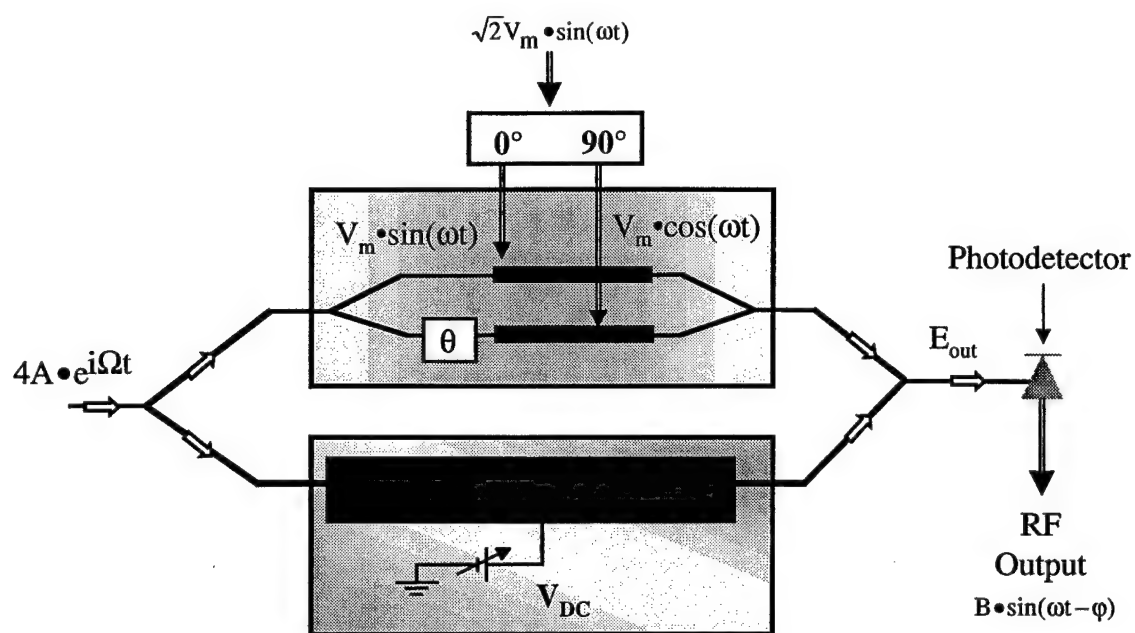
9

systems. Mechanical support for the device was provided by a silicon wafer, on which the microstrip ground was deposited. The microstrip ground consisted of a thin Cr layer used for adhesion followed by a layer of Au. Following deposition of the ground the lower cladding and active layer were spin coated and subsequently the partially completed device was corona poled. The active polymer used in the PPS was CLD2, which exhibited an electro-optic coefficient of 37 pm/V at 1.06 μm and it is a member of a family of large electro-optic coefficient materials. The optical rib waveguides were then patterned using RIE. The PPS was completed by spinning the upper cladding and depositing a 4 μm thick Au strip using the procedure outlined in the previous section. This strip thickness was chosen to minimize microstrip loss. A picture of an array of completed devices is shown in Figure 5b. This fabrication procedure was similar to the one described in the previous section, in which it was demonstrated that a Mylar substrate could be integrated into the device without significant process alteration.

As part of our phase I effort we also conducted extensive modeling of the PPS shown in Figure 5a. This device implemented the microwave phase shift as follows. An optical field of amplitude 4A and frequency Ω formed the optical input to the primary Mach-Zehnder. Part of this field was routed to the secondary Mach-Zehnder whose arms were driven in quadrature by the microwave field of frequency ω and amplitude V_m. Furthermore, one of the secondary Mach-Zehnder arms experienced an additional θ phase delay ($\theta = \pi/2$ to perform a single side-band frequency shift). The remainder of the optical field was routed to the other arm of the primary Mach-Zehnder where the field developed a phase shift in response to the DC or quasi-DC potential. It was this potential that controlled the phase, φ, of the detected microwave field. Upon illumination of the photodetector, the resulting photocurrent, $i_p(\omega)$, was proportional to the intensity modulated at ω and it was given by
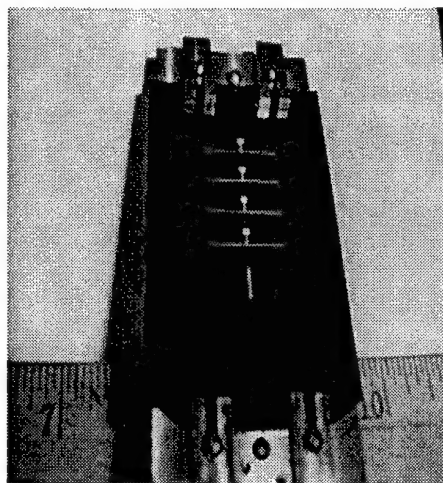
$$
\begin{aligned}
i_p(\omega) \propto & \left[4J_1\left(\frac{\pi V_m}{V_\pi}\right) \cdot \sin\left(\frac{\pi V_{DC}}{V_\pi}\right) + \sqrt{2}J_1\left(\sqrt{2}\frac{\pi V_m}{V_\pi}\right) \cdot \sin\left(\frac{\pi V_\theta}{V_\pi}\right) \right] \sin\omega t \\
& + \left[4J_1\left(\frac{\pi V_m}{V_\pi}\right) \cdot \sin\left(\frac{\pi V_{DC}}{V_\pi} - \frac{\pi V_\theta}{V_\pi}\right) - \sqrt{2}J_1\left(\sqrt{2}\frac{\pi V_m}{V_\pi}\right) \cdot \sin\left(\frac{\pi V_\theta}{V_\pi}\right) \right] \cos\omega t
\end{aligned}
\tag{2}
$$

$$
= B \cdot \sin(\omega t - \varphi)
$$

In (1) $J_1(x)$ was the first order Bessel function of the first kind, V_θ was the voltage required to generate an optical phase of θ, and V_π was the half-wave voltage for each arm of the PPS. Under normal operating conditions the microwave phase shift was given by

$$
\varphi(V_{DC}, V_m) = \tan^{-1}\left(\frac{4J_1\left(\frac{\pi V_m}{V_\pi}\right) \cdot \cos\left(\frac{\pi V_{DC}}{V_\pi}\right) + \sqrt{2}J_1\left(\sqrt{2}\frac{\pi V_m}{V_\pi}\right)}{4J_1\left(\frac{\pi V_m}{V_\pi}\right) \cdot \sin\left(\frac{\pi V_{DC}}{V_\pi}\right) + \sqrt{2}J_1\left(\sqrt{2}\frac{\pi V_m}{V_\pi}\right)} \right).
\tag{3}
$$

Figure 5. a) Schematic representation of the photonic phase shifter investigated during our phase I effort and b) picture of fabricated phase shifter array.

The microwave phase shift characteristics as given by equation (3) were investigated assuming $V_\pi = 10.8$ V and V_{DC} varying linearly between –3.9 and 3.9 V. For a 15 dBm microwave launched into the 50 Ω microstrip lines of the RF PPS, a maximum microwave phase difference of 82° was calculated. Furthermore, the calculated microwave phase varied nearly linearly with respect to V_{DC} for the specified conditions and exhibited a slope of 10.5°/V. A linear characteristic is highly desirable because it can significantly simplify the circuitry controlling the RF PPS. As observed in (3) the microwave phase also depended on the amplitude of the microwave field. Consequently, it was significant to determine the microwave power range over which φ was primarily controlled by V_{DC}. This microwave power range was estimated by comparing equation (2) to the microwave phase calculated for the small microwave drive case. A microwave power range between –30 to 21 dBm was observed over which the microwave phase was primarily controlled by V_{DC}. Therefore, the fabricated RF PPS architecture was expected to produce nearly 100° degrees phase shift with a nearly linear characteristic.

The PPS characterization system is shown in Figure 6. An Nd:YAG laser operating at 1310 nm was butt coupled to the PPS optical waveguide using single mode PM fiber. Port 1 of a HP 8510 network analyzer was used as the microwave source, which was subsequently divided in two by a 3 dB power splitter. The lengths of both microwave arms were precisely adjusted so as to obtain components in quadrature at their outputs. Air spaced microwave probes were used to launch the microwave field into the PPS microstrip lines. A bias tee was used to provide V_θ to one of the microstrip lines while a DC probe was used to provide V_{DC} to the phase control pad. The PPS output was incident on a large bandwidth photodetector, whose output was sent to Port 2 of the network analyzer for phase comparison with the source at Port 1.
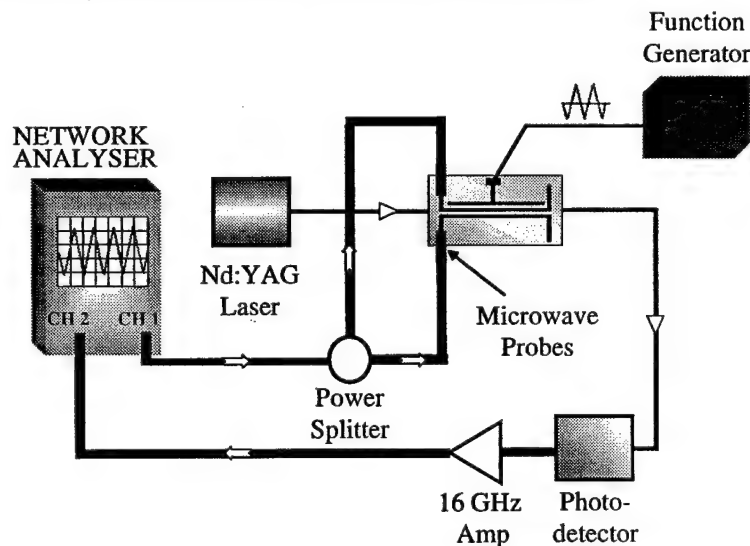

Figure 6. Photonic phase shifter characterization setup. In this case a network analyzer was used to compare the phase of the detected signal to that driving the PPS.

The PPSs fabricated during our phase I effort and shown in Figure 5b were characterized using this setup with $\theta = \pi/2$. In this case a HP function generator was used to drive the DC control pad with a 50 Hz triangular wave of 3.9 V amplitude, shown in Figure 7a.
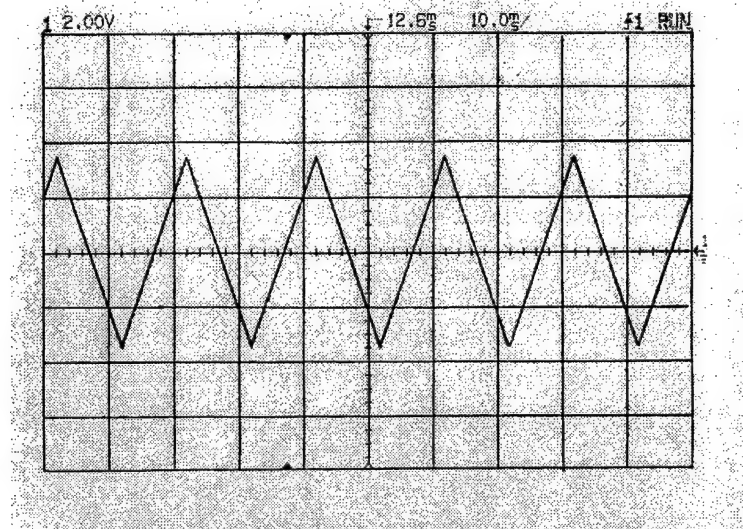
a)
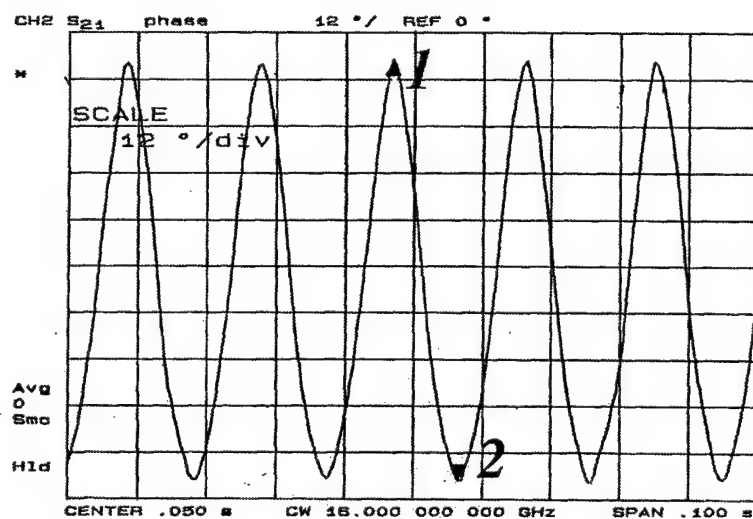
1: 41.3°   2: -66.8°

b)

Figure 7. a) 7.8 V peak-peak 50 Hz triangular waveform applied to the DC control pad. b) Phase of 16 GHz detected signal as measured by port 2 of the network analyzer. A maximum phase difference of 108.1° was measured.

These devices exhibited a $V_\pi = 10.8$ V. For a 15 dBm microwave signal at 16 GHz and the control voltage shown in Figure 7a, the measured microwave phase is shown in Figure 7b. A maximum phase difference of 108.1° was measured. Furthermore, the microwave phase varied nearly linearly with V_{DC} and exhibited a slope of 13.9°/V. All these results were in reasonable agreement with the results predicted by our calculations. As seen from (2) the amplitude of $i_p(\omega)$ was a function of V_m, V_θ, and V_{DC}. Under the conditions of this experiment the detected microwave power varied by more than 6 dB over the range of V_{DC}. These initial results were highly encouraging because they demonstrated the potential for high performance polymeric PPSs.

The phase shifting structure shown in Figure 5a has another significant advantage it is addressable. That is the output of the PPS can be enabled and disabled by appropriately choosing V_θ and V_{DC}. If $V_\theta = nV_\pi$ and $V_{DC} = mV_\pi$ then from equation (1) the photocurrent, $i_p(\omega)$, is identically zero. Operation of the PPS in this mode will be termed disabled mode. If, on the other hand $V_\theta = .5V_\pi$ and V_{DC} is allowed to take on any value then the shifter is enabled. This enabling/disabling function may prove useful in pulsed photonic phased array radars where an addressable PPS can eliminate the need for any additional RF switching elements. The implementation of flexible PPS in complex systems will be addressed later. In order to determined the usability of the addressing function, investigations of the photocurrent amplitude as a function of V_θ will be conducted.

In summary, during our phase I effort we employed our mature polymer fabrication techniques in the realization of an RF PPS, which was subsequently modeled and tested. These initial results were highly encouraging for they demonstrated the feasibility of high performance polymeric PPSs. The push for lightweight photonically controlled circuitry used in smart skin and conformal structures provides the emphasis for the future development of a flexible RF photonic phase shifter. Polymeric fabrication techniques are already in place that can meet this demand. Of particular importance are the characterization of the flexible PPS under flexed conditions and the impact of optical and microwave waveguide bending. These investigations will allow the full realization of the potential of the device conformal properties. Furthermore, the present RF PPS configuration investigated exhibits addressable properties. This is an advantage of the present RF PPS architecture, which can have a significant impact on complex system design. Therefore, the addressing or enabling/disabling function must be accurately characterized.

3. Microwave Crosstalk Measurements of Closely Spaced Polymer Modulators

High-density arrays of high-speed modulators are of significant importance for a variety of applications, which include optical RF distribution and optical interconnects. RF isolation is an important consideration in commercially packaged modulator arrays and limits the number of active modulators on a single chip that can be packaged. High

14

speeds and improved r_{33} have enabled polymer materials to become competitive when compared to $LiNbO_3$. However, in addition to higher individual device performance, modulator arrays are required to exhibit small crosstalk levels. During current investigations characterization of a FTC Mach-Zehnder modulators and subsequent crosstalk measurements of a packaged modulator arrays on rigid substrates were performed. For devices separated by 400 μm a −50 dB crosstalk level was measured across a 20 GHz band. These results are impressive considering that no crosstalk reduction techniques, such as buried microstrip lines, were implemented. Comparable results are anticipated for devices fabricated on flexible substrates.

Two sets of measurements have been made on unpackaged devices. The first involved measurement of the microwave crosstalk between two adjacent microstrip lines spaced 400 μm apart. The schematic of the measurement is shown on Figure 8. A Coplanar probe was used to launch the microwave signal at 1 and another probe was used to measure the signal at point 3 or 4. An 8510 Network Analyzer was used to determine the crosstalk as a function of frequency up to 40 GHz. A measurement made between points 1 and 3 is referred to as the 'Near-end crosstalk' was measured to be less than −40 dB (power) over the entire band of 0-40 GHz. The next measurement involved a measurement of the modulation crosstalk between the adjacent modulators. Light was launched in the optical waveguide of one of the modulators and the microwave was launched first in the microstrip of the same modulator and then in the microstrip line of an adjacent modulator. Optical heterodyne was used to detect the modulation in either case. A signal to noise of 30 dB was obtained in the first case while no modulation signal could be observed in the latter case.
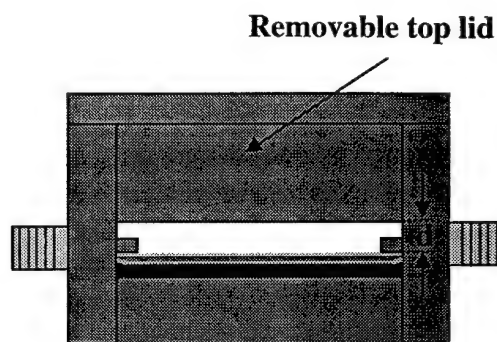
A set of crosstalk measurements was also made on a FTC modulator that was packaged. Two adjacent microstrip lines (400 μm apart) at the center of the chip were fitted with K connectors on either end. The schematic of the packaging is shown in Figure 8. The modulator was enclosed in a metal case with a removable top lid. Lids of three different thicknesses were designed so as to adjust the lid-device spacing to 3, 5.5 and 7 mm. This was done to study the dependence of crosstalk on the packaging parameters. The device was cleaved close to the tapered ends of the electrodes. The polymer on either side of the tapered section was removed so as to expose the lower ground plane. Silver epoxy was used to connect the exposed ground to the metal body of the package (ground) and also the microstrip line to the center pin of the K-connector. The epoxy was cured at 50 °C for a period of 48 hours. The photograph of the packaged device with and without the top lid is shown in Figure 9.

The connector to connector transmission measurement on the Network Analyzer showed a drop to about −23 dB at a frequency of 20 GHz. This is mainly attributed to the loss in the taper and the bends in the microstrip lines. Crosstalk measurements were also made on adjacent packaged lines. The far-end crosstalk (refer Figure 10) was seen to be below −55 dB over the 0-20 GHz frequency band, which partially reflects measured microwave insertion losses. The high RF isolation in our polymer modulators makes it possible to realize closely spaced, large modulators arrays that would have widespread applications in communications and phased array systems.

Microstrip lines

2   3

400 µm

4   1

Removable top lid
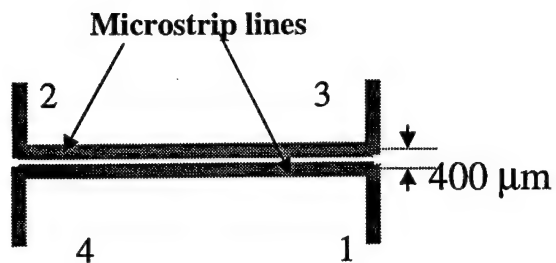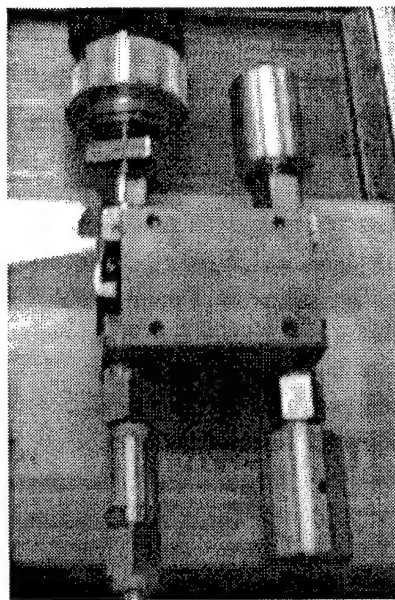
Schematic of crosstalk measurements   **Side view of the packaged device**

Figure 8. Schematic of the packaged FTC modulator. Silver epoxy is used to make contact of the center pin of the K connector to the top electrode of the line. The bottom ground electrode of the line is grounded to the metal body of the package (d is the distance between device and the top lid).
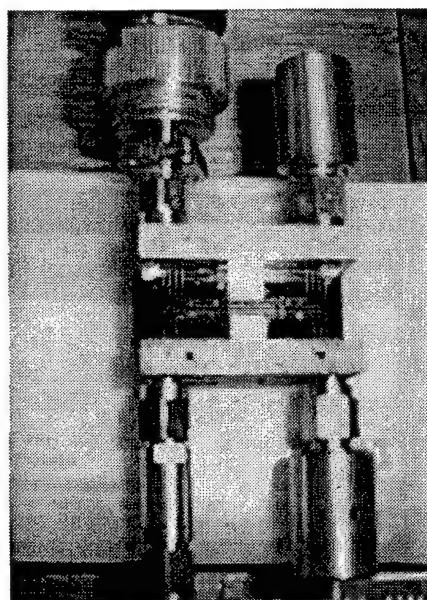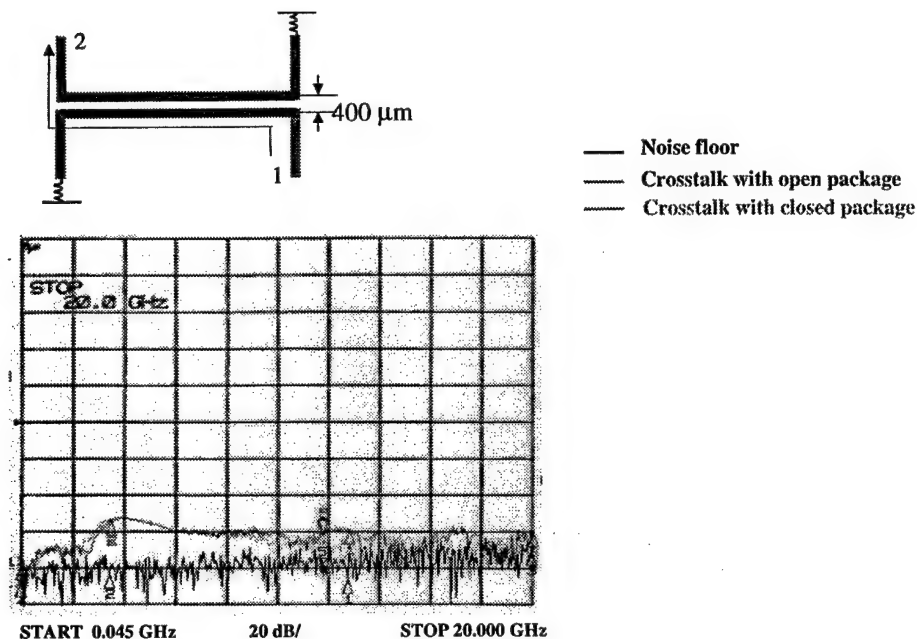

Open packaging   **Closed packaging**

Figure 9. Photograph of the packaged modulator with and without the top lid.

16

Figure 10. Far-end crosstalk measurements for the packaged modulator. The effect of the packaging (presence of the top lid) on the crosstalk between adjacent lines does not seem to be significant. The maximum crosstalk is less than –55 dBm.

4. Computer Simulation of Complex Three-Dimensional Optical Waveguide Structures on Flexible Substrates

In the past, PWI and USC had used a commercial computer program named BeamPROP from RSoft for designing the optical structures of our polymer modulators. This CAD program is specially written for design and simulation of photonic integrated circuits. For multi-layered two-dimensional (2.5 D) structures, BeamPROP can generate accurate results for guided modes within a few minutes. However, it assumes all layers are infinitely wide and cover layers are infinitely thick. Because of these assumptions, BeamPROP is not capable of solving cladding modes and their coupling with guided modes. Also, all layers are assumed to be flat in its calculation. Consequently, it is not suitable for simulating bent modulators.

In order to simulate the effects of bending on polymer modulators, a true three-dimensional electromagnetic (EM) simulator is needed. During our Phase I effort, we have chosen the commercial software from Hewlett Packard, namely the High-Frequency Structure Simulator (HFSS), for our purposes. Originally intended for microwave component designers, HFSS offers an intuitive drawing environment, a powerful finite-element EM simulator, and robust display capabilities. The major advantages of this software are: (1) analysis based solely on Maxwell's equations, and (2) unrestricted geometries and unlimited number of dielectrics and conductors. However, due to its

17

brute force finite-element techniques, HFSS requires a large amount of memory and CPU time to solve any practical structures. This is especially true when it is used for photonic component simulation because of the existence of multiple cladding modes. Examples of these modes in a polymer modulator will be shown later.

During the Phase I effort, we have successfully simulated the effects of a five-degree bending on a polymer modulator waveguide. The cross section view of the simulated structure is shown in Figure 11. The bend was assumed to span for 1.3 μm. Due to the finite dimensions in the transverse directions, the structure supports both desired guided modes and many unwanted cladding modes. Figure 12 shows the first 5 and the 19th modes. To confirm the accuracy of HFSS for this application, we first simulated the structure without any bending and compared the so calculated propagation constants of the guided modes to those using BeamPROP. The two programs provided similar results as expected. Because of the relative small ridge height, HFSS needed many iterations to converge to acceptable accuracy. In this preliminary calculation for the bent modulator, we assumed a pure mode #1 excitation on the input port and only considered the scattering between the first 5 modes to save memory and time. After 42 iterations, the results show that less than 0.5 % of the optical power is reflected back or scattered into higher order modes. Table 1 lists the reflection and transmission of the first 5 modes. Based on this data, we predict the five-degree distortion has negligible effects on the optical performance.
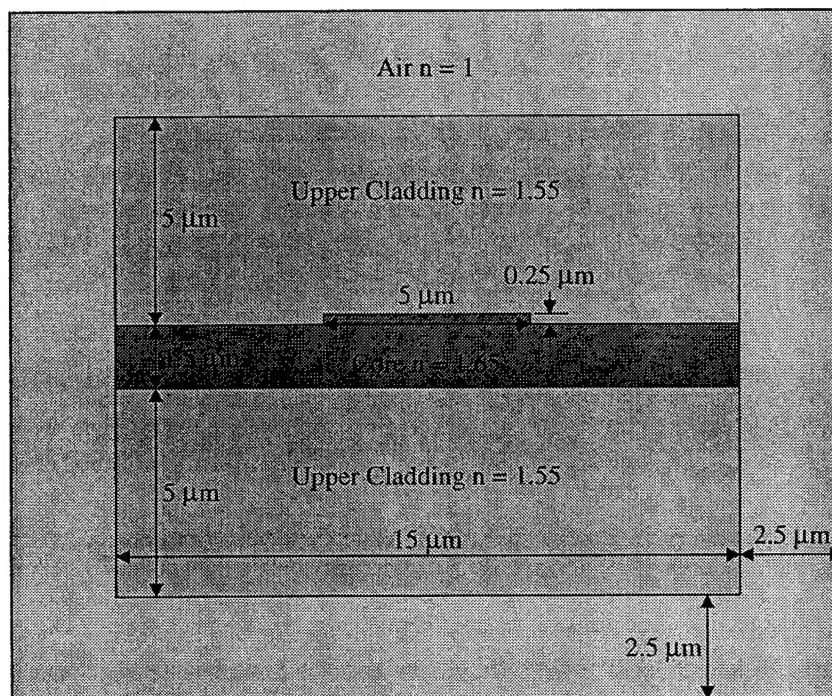

Figure 11. The cross section view of the simulated structure. It is assumed to be surrounded by perfect conductors.

18

Table 1. The calculated reflection and transmission under pure fundamental mode excitation.

Mode No.	1	2	3	4	5
Reflected Power (%)	0.24	0.02	0.04	0.01	0.04
Transmitted Power (%)	99.57	0.02	0.01	0.00	0.04

The above mentioned simulation was carried out using a 400 MHz Pentium II processor with 384 MB of memory. This calculation took over 48 hours to complete. That was the main reason that only a five-degree bending and the first five modes were considered. To be able to simulate larger and different types of distortion, and to improve the accuracy by incorporating more modes, PWI has recently purchased a new workstation with two 500 MHz Pentium III processors and 1 GB of memory. This system will be used extensively in our Phase II effort to optimize the flexible modulator design.
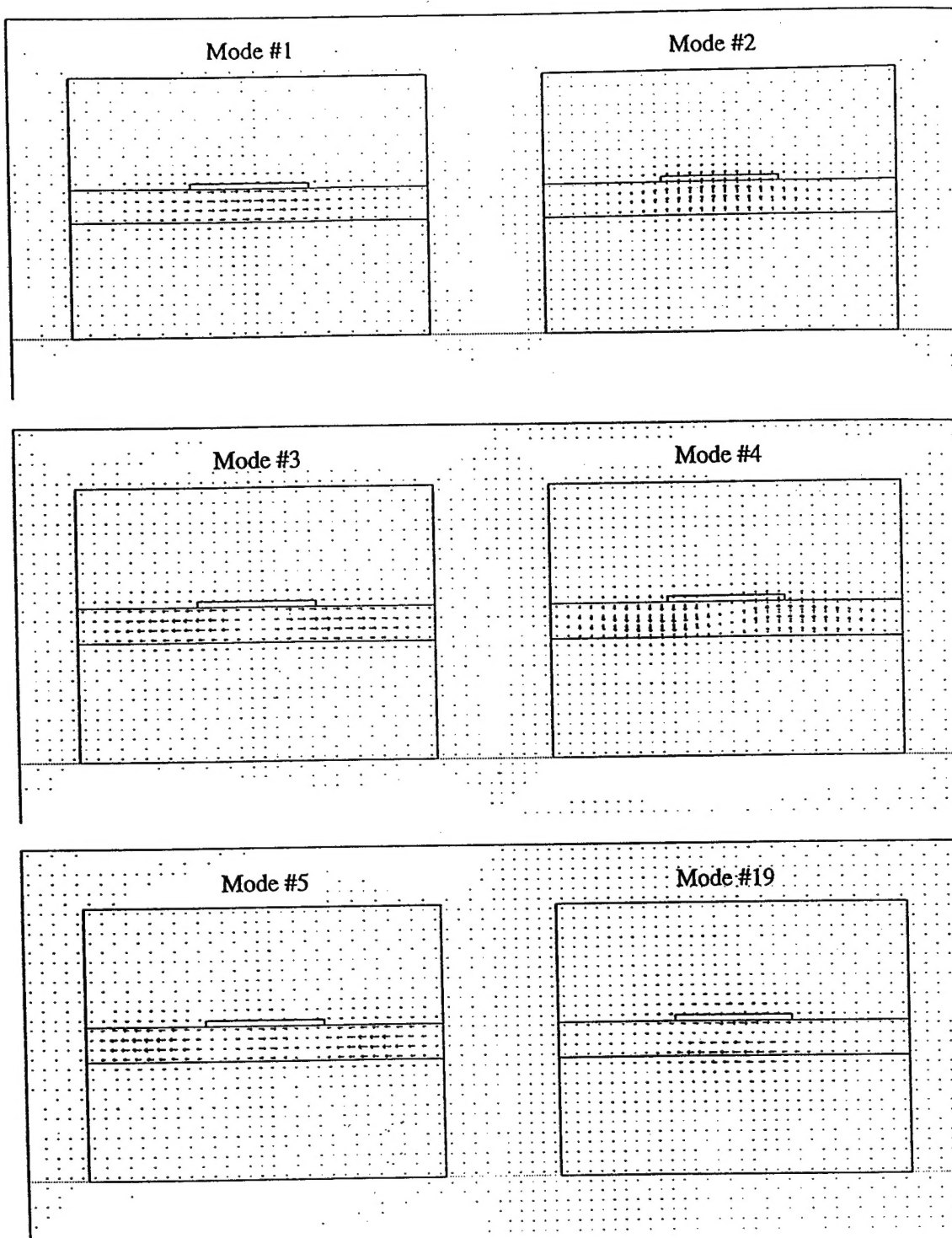
Figure 12. The electric field distribution of the first 5 and the 19th modes.

Conclusion

In this Phase I research PWI and USC successfully fabricated and tested polymer amplitude modulators on Mylar substrate at W-band frequencies. Our polymer materials and device fabrication technology were extended to flexible dielectric substrates, which may lead to major innovations in optically controlled conformal antenna arrays. Traveling wave electro-optic modulators were demonstrated on flexible substrates with integrated finline microstrip-to-rectangular waveguide transitions without any degradation of their performance. This will allow us to extend our commercialization efforts to modulators working at W-band frequencies utilizing these finline transitions. The actual packaging of the ultra-high frequency polymer modulators (up to 100 GHz) is under way.

In addition, we realized RF Photonic Phase Shifter, which was subsequently modeled and tested. It consisted of two nested Mach-Zehnder structures and allowed over 100^0 of near linear phase shift of 16 GHz microwave signal at DC control voltage change of 7.9 V. These initial results are highly encouraging for they demonstrate the feasibility of high performance polymeric PPSs. Furthermore, the present RF PPS configuration exhibits addressable properties. This is an advantage of that particular RF PPS architecture, which requires further accurate characterization.

It is our current plan to continue this effort that will have an important role in supporting new architectures of optically controlled conformal antenna arrays. We intend to evaluate the design, fabrication, and performance of several types of photonic devices on flexible substrates. These devices include integrated polymer optical modulators, photonic RF phase shifters, and photonic switches. These constitute main building blocks for large area steerable antenna structures. We anticipate that successful completion of Phase II effort will see the development of commercially viable arrays of flexible modulators and photonic phase shifters.